Measurement of Interference between W and Z Exchange in Electron-Neutrino Electron Scattering

R. C. Allen,[a] H. H. Chen,[b] P. J. Doe,[c] R. Hausammann,[d] W. P. Lee,[e] H. J. Mahler,[f] M. E. Potter,[c] X. Q. Lu,[g] and K. C. Wang[g]
University of California, Irvine, California 92717

T. J. Bowles, R. L. Burman, R. D. Carlini,[h] D. R. F. Cochran, J. S. Frank,[i] E. Piasetzky,[j] and V. D. Sandberg
Los Alamos National Laboratory, Los Alamos, New Mexico 87545

D. A. Krakauer[k] and R. L. Talaga[k]
University of Maryland, College Park, Maryland 20742
(Received 13 November 1989)

A measurement of the reaction $\nu_e + e^- \rightarrow \nu_e + e^-$ was performed using a beam-stop source of ν_e. Based upon 234 ± 35 events, we obtain a cross section of $\sigma(\nu_e e) = [9.9 \pm 1.5(\text{stat}) \pm 1.0(\text{syst})] \times 10^{-42}$ cm$^2 \times [E_\nu$ (GeV)]. This reaction is mediated by the exchange of W and Z bosons and is thus sensitive to the interference between them. This interference is measured to be $-1.07 \pm 0.17(\text{stat}) \pm 0.11(\text{syst})$, consistent with the destructive interference (-1.08) predicted by the standard model.

PACS numbers: 13.10.+q, 12.15.Ji, 14.80.Er

The elastic-scattering reaction, $\nu_e e \rightarrow \nu_e e$, first observed in 1985,[1] is mediated via both the charged-current and neutral-current interactions, in contrast to the neutral-current reactions $\nu_\mu e \rightarrow \nu_\mu e$ and $\bar{\nu}_\mu e \rightarrow \bar{\nu}_\mu e$. If the outgoing neutrino from the charged-current interaction is the same as the outgoing neutrino from the neutral-current interaction, then these two interactions will interfere. The cross section for the reaction $\nu_e e \rightarrow \nu_e e$ can be written as the sum of a neutral-current term, a charged-current term, and an interference term between charged and neutral currents.[2] Assuming μ-e universality, the neutral-current term is equal to $\sigma(\nu_\mu e)$, which has been measured by several experiments,[3,4] and the charged-current term is defined to be $2G_F^2 m_e E_\nu/\pi$, where the Fermi constant G_F is measured by muon-decay experiments, and E_ν is the laboratory energy of the incident neutrino. The interference term can be expressed as $IG_F^2 m_e E_\nu/\pi$, where I measures the interference strength. Thus, the sign and magnitude of the interference between charged- and neutral-current amplitudes can be deduced from an accurate measurement of the $\nu_e e$ cross section. A similar reaction, $\bar{\nu}_e e \rightarrow \bar{\nu}_e e$, has been observed,[5] although with insufficient accuracy to measure an interference effect.

In the Weinberg-Salam-Glashow (WSG) model of electroweak interactions,[6] the neutral-current interaction is mediated by the Z boson, and the charged-current interaction by the $W^\pm$ bosons. A destructive value of the interference is predicted ($I_{\text{WSG}} = -2 + 4\sin^2\theta_W$) that lowers the $\nu_e e$ cross section by 40% compared with that in the absence of interference.

This experiment used the intense flux of ν_e available at the proton beam stop of the Clinton P. Anderson Meson Physics Facility (LAMPF) at the Los Alamos National Laboratory. These neutrinos are produced mostly from stopped π^+ decays, which make 30-MeV ν_μ, followed by stopped μ^+ decays, which make $\bar{\nu}_\mu$ and ν_e with endpoint energies of 53 MeV; the mean ν_e energy is 31.7 MeV. For our 20-MeV electron detection threshold, the recoil electron from $\nu_x e$ scattering (where ν_x refers to any of the above three types of neutrinos) is confined within a 10° cone with respect to the incident neutrino direction. Thus, the elastic-scattering signal is forward peaked, whereas backgrounds from both cosmic rays and the accelerator are essentially isotropic.

Details of the detector have been previously published.[1,7] Briefly, a system of active and passive shielding surrounds a 15-metric-ton central tracking detector. The active shield, which consists of 594 multiwire proportional counters arranged in four layers that cover all surfaces of the detector, is used to reject incoming charged particles. Within the active shield, a 100-g/cm^2 layer of steel and lead is used to convert and attenuate residual γ's from cosmic-ray muons. The fine-grained central detector is used to measure the energy and track direction of the recoil electrons. It is arranged in a sandwich structure of forty identical layers. Each 305-cm-high-by-305-cm-wide layer consists of four pieces of 76-cm-wide-by-2.5-cm-thick plastic scintillator, each viewed by a single 12.7-cm-diam photomultiplier tube. Each scintillation layer is followed by ten panels of flash chambers, each containing 520 polypropylene flash tubes filled with a mixture of helium-neon gas, arranged in alternating X and Y planes. The total number of target electrons in the central detector is $(4.94 \pm 0.05) \times 10^{30}$.

The LAMPF beam macrostructure typically consists of a 0.75-ms beam spill followed by a 7.58-ms beam-off interval. During the beam-off interval, a beam-off gate is opened in order to collect cosmic-ray backgrounds. The beam-off gate is typically 3 times longer than the

beam-on gate in order to reduce the statistical uncertainty of the cosmic-ray background determination. The total beam exposure was 1.12×10^{23} protons (4.96 Ah). To provide ongoing detector calibrations, through-going muons and stopped-muon decays are collected every 5 min. These calibration data are used to measure the pedestals and gains of each channel as a function of time and to monitor the performance of the flash-chamber system.

The detector is triggered by a coincidence between at least three contiguous scintillation layers, with an energy deposition of between 1 and 18 MeV per plane, and no veto from the active shield. A veto is defined as hits in two out of the four proportional-counter layers in the walls or roof, resulting in a veto rate of 6 kHz. The detector is blocked for 20 μs after each veto to prevent triggers by electrons from stopped-muon decay, resulting in a dead time of 13%.

The trigger rate of less than 0.1 Hz is dominated by cosmic-ray and accelerator backgrounds. To reduce these backgrounds, restrictions are imposed on the data. First, cosmic-ray events are eliminated by removing events with substantial activity in the active shield, or in the scintillation counters during the 32 μs preceding the trigger. Next, a fiducial region excluding the outer 5 cm of the detector is defined in order to remove γ's that converted in the inner shield. This restriction also removes incoming charged particles not identified by the active shield and insures that the remaining events are completely contained within the central detector. The combination of enhanced veto efficiency and better geometric definition gives a factor-of-9 reduction in background while retaining 70% of the neutrino-electron triggers.

Nonelectron backgrounds are reduced by removing events with a dE/dx greater than 4 MeV/cm (twice minimum ionizing) in any layer and events with less than 12 MeV/cm in any middle layer. Events with more than two clusters of adjacent scintillators, or with a poor-quality fit to a track, are assumed to be associated with low-energy neutrons, and are eliminated. The improved electron identification removes an additional 9% of the neutrino-electron triggers but gives a further reduction of 4 in backgrounds. The resulting overall reduction by 36 in the background level leaves 4880 events in the beam-spill period. Finally, the 12953 events taken during the beam-off gate are used to determine and then to subtract the cosmic-ray background, leaving a total of 1492 ± 76 beam-associated electron events. The observed energy and angular distributions of these recoil electrons are shown in Figs. 1 and 2, respectively.

A multiparameter fit to the two-dimensional distribution of recoil angle versus observed energy is used to determine the elastic-scattering signal. The components of the fit are given by the Monte Carlo expectations for the background and signal shapes. The overall normalization of each distribution is allowed to vary with the total number of events fixed. The distributions used in the fit correspond to $\nu_x e$ elastic scattering, ν_e ^{12}C and ν_e ^{13}C inverse β decay,[8] and neutron-induced background. The ν_e ^{13}C distributions represent the combination of all neutrino-nuclei interactions in the detector with low threshold values (^{13}C, ^{27}Al, ^{35}Cl). The fit to the observed energy and angular distributions is shown as solid lines in Figs. 1 and 2. This fit results in a measurement of 295 ± 35 $\nu_x e$ events, 626 ± 71 ν_e ^{12}C events, and 571 ± 136 remaining background events of which ap-

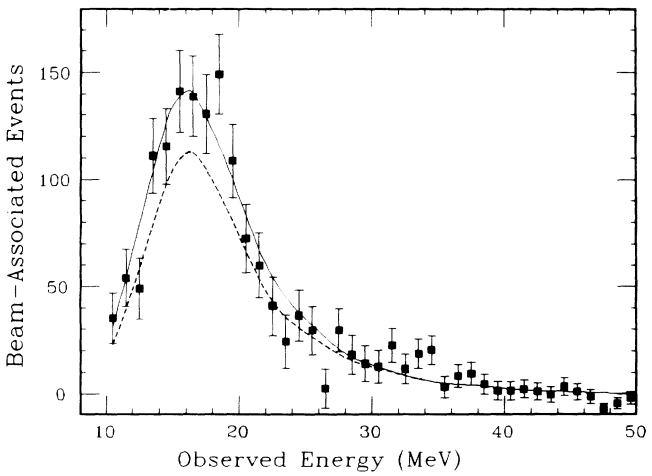

FIG. 1. The observed energy spectrum of the beam-associated recoil electrons. Because of the presence of the flash chambers, only about $\frac{2}{3}$ of the total particle energy is deposited in the scintillators. The solid line indicates the fit to the Monte Carlo distributions for the expected signal and backgrounds. The dotted line indicates the background only.

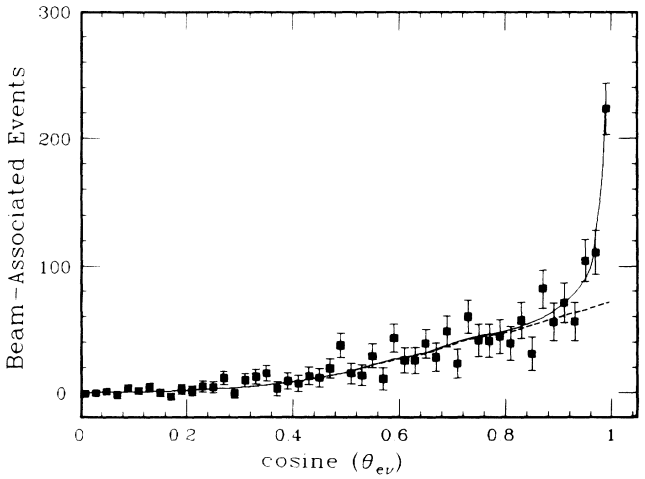

FIG. 2. The angular spectrum of the beam-associated recoil electrons. Here, $\theta_{e\nu}$ is the angle between the incident neutrino and the reconstructed recoil electron. The solid line indicates the fit to the Monte Carlo distributions for the expected signal and backgrounds. The dotted line indicates the background only.

proximately 140 are expected from other neutrino-nuclei interactions, and the remainder attributed to neutron-induced backgrounds. In addition, the $\nu_e\,{}^{12}\mathrm{C}\rightarrow e^-\,{}^{12}\mathrm{N}$(g.s.) reaction, which is the main source of beam-associated background, was simultaneously measured by detection of the delayed positron from the ${}^{12}\mathrm{N}\rightarrow{}^{12}\mathrm{C}e^+\nu_e$ β decay; this measurement[9] gives results consistent with the distribution fit.

The Monte Carlo simulation used to simulate the energy and angular distributions for the above fit is also used to compute the detector efficiency for recoil electrons. This simulation, based upon the electron-gamma-shower code (EGS4), takes into account light attenuation in the scintillators and photoelectron statistics. The flash-chamber system is modeled in the Monte Carlo program, and is calibrated using through-going muon events. Noise in the scintillators, flash chambers, and proportional counters is taken from through-going muon events and randomly added to the Monte Carlo events. Events generated by the Monte Carlo simulation are passed through the same data-reduction and analysis programs that are used for the actual data. To check this procedure, stopped-muon decay electrons are simulated and are in excellent agreement with measured data as shown in Figs. 3 and 4.

The systematic uncertainty in the recoil-electron detection efficiency is evaluated by measuring the sensitivity of the Monte Carlo simulation to changes in input parameters and simulation algorithms. Uncertainties in the detector energy scale (2.5%), flash-chamber performance (4.0%), and random noise rate (1.5%) lead to a combined systematic uncertainty of $\pm 5\%$ in the detection efficiency. The overall detection efficiency for $\nu_e e$ scattering is found to be $(16.5\pm 0.8)\%$.

The largest systematic error comes from uncertainty in the neutrino flux from the beam stop. An experiment (E866) to measure the number of stopped π^+ decays followed by stopped μ^+ decays per incident proton in an instrumented beam stop of various materials was performed at LAMPF.[10] These results were used to calibrate a Monte Carlo program[11] that provided a detailed simulation of the actual proton beam stop at LAMPF. The estimated error of 7.3% in the neutrino flux calculated by the Monte Carlo program comes from six sources: systematic effects in the E866 measurement (5.9%), normalization of the Monte Carlo code to the six separate absolute measurements of E866 (2.4%), simulation of the full LAMPF beam stop (3%), the proton beam energy (0.3%), the absolute proton flux (2%), and the distance from source to detector (0.5%). For our entire beam exposure, the total resulting time-integrated neutrino flux is computed to be $(9.16\pm 0.67)\times 10^{14}\,\nu_e/\mathrm{cm}^2$, at the average detector distance from the beam stop of 898 cm. When the uncertainty in the flux and the detection efficiency are added in quadrature, the total systematic uncertainty is 8.8%.

The 295 ± 35 neutrino-electron events include contributions from $\nu_\mu e$ and $\bar{\nu}_\mu e$. Using measured cross sections from previous experiments,[3,4] 27.4 ± 4.7 $\nu_\mu e$ and 33.5 ± 5.9 $\bar{\nu}_\mu e$ events are subtracted, leaving 234 ± 35 $\nu_e e$ events; in the absence of interference, 448 ± 40 $\nu_e e$ events would be expected. From the 234 $\nu_e e$ events, the total cross section is

$$\sigma(\nu_e e)=[9.9\pm 1.5(\mathrm{stat})\pm 1.0(\mathrm{syst})]\times 10^{-42}\,\mathrm{cm}^2\times[E_\nu\,(\mathrm{GeV})]$$

or $\sigma(\nu_e e)=(1.15\pm 0.21)G_F^2 m_e E_\nu/\pi$. The charged-cur-

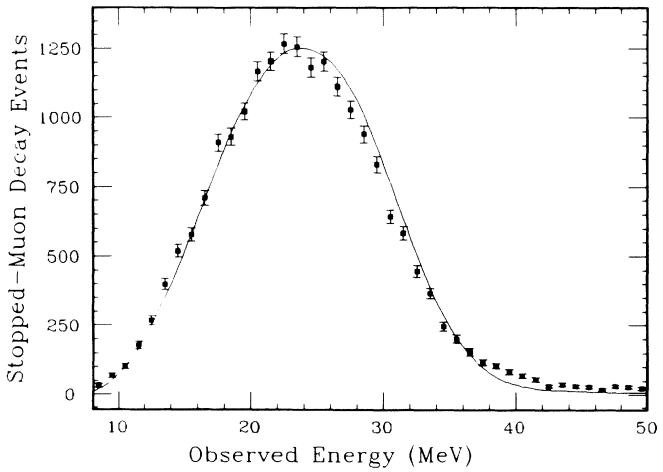

FIG. 3. The observed energy spectrum of electrons from stopped-muon decay. The solid line indicates the expectation from the Monte Carlo simulation.

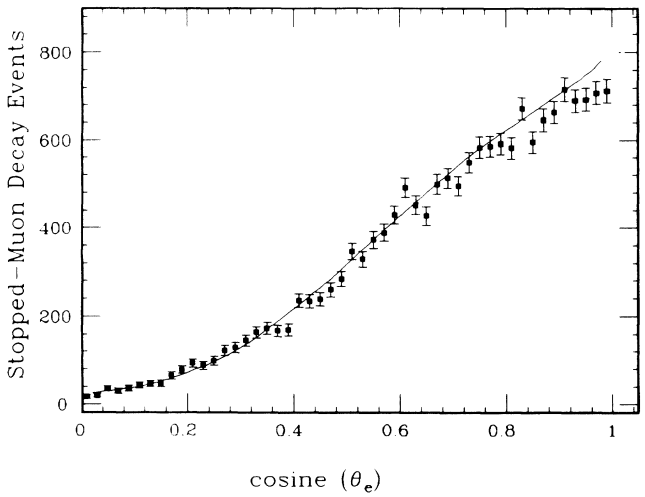

FIG. 4. The observed angular spectrum of electrons from stopped-muon decay. Here, θ_e is the laboratory angle of the reconstructed electron. The solid line indicates the expectation from the Monte Carlo simulation.

rent contribution to this cross section is $2G_F^2 m_e E_\nu/\pi$. From the muon-neutrino electron elastic-scattering experiments,[3,4] the neutral-current contribution is measured to be $(0.22 \pm 0.03) G_F^2 m_e E_\nu/\pi$. By subtracting the charged- and neutral-current contributions from the measured $\nu_e e$ cross section the interference strength is determined to be

$$I = -1.07 \pm 0.17(\text{stat}) \pm 0.12(\text{syst}) .$$

For $\sin^2\theta_W = 0.230$ (world average[12]), the standard model predicts a value of $I_{\text{WSG}} = -1.08$.

In conclusion, we have measured the $\nu_e e \rightarrow \nu_e e$ cross section to sufficient precision (18%) to determine the interference between W and Z exchange. This first measurement of the sign and magnitude of the coherent interference is in excellent agreement with the predictions of the WSG electroweak model.

This experiment has received much encouragement and support from the University of California, Irvine, the Los Alamos National Laboratory, and the University of Maryland. In particular, we thank N. Briscoe, J. Sena, T. N. Thompson, S. DeLay, and many others at these institutions for their efforts on our behalf. This work is supported in part by the U.S. National Science Foundation under Grant No. PHY-8501559 and by the U.S. Department of Energy.

---

[a]Now at Hewlett-Packard Laboratories, Palo Alto, CA 94304.
[b]Deceased.
[c]Now at Los Alamos National Laboratory, Los Alamos, NM 87545.
[d]Now at University of Geneva, Geneva, Switzerland.
[e]Now at Jet Propulsion Laboratory, Pasadena, CA 91109.
[f]Now at Cerebus AG, Mannedoff, Switzerland.
[g]Now at Rockwell International, Thousand Oaks, CA 91360.
[h]Now at Continuous Electron Beam Accelerator Facility, Newport News, VA 23606.
[i]Now at Brookhaven National Laboratory, Upton, NY 11973.
[j]Now at Tel Aviv University, Ramat Aviv, Israel.
[k]Now at Argonne National Laboratory, Argonne, IL 60439.

[1]R. C. Allen *et al.*, Phys. Rev. Lett. **55**, 2401 (1985).
[2]B. Kayser *et al.*, Phys. Rev. D **20**, 87 (1979).
[3]J. Dorenbosch *et al.*, Z. Phys. C **41**, 567 (1989).
[4]K. Abe *et al.*, Phys. Rev. Lett. **62**, 1709 (1989).
[5]F. Reines, H. S. Gurr, and H. W. Sobel, Phys. Rev. Lett. **37**, 315 (1976); G. S. Vidyakin *et al.*, Pis'ma Zh. Eksp. Teor. Fiz. **49**, 646 (1989) [JEPT Lett. **49**, 740 (1989)].
[6]S. Weinberg, Phys. Rev. Lett. **19**, 1264 (1967); A. Salam, in *Elementary Particle Theory,* edited by N. Svartholm (Almquist and Wiksell, Stockholm, 1968), p. 367; S. L. Glashow, Nucl. Phys. **22**, 579 (1961).
[7]R. C. Allen *et al.*, Nucl. Instrum. Methods Phys. Res., Sect. A **269**, 177 (1988).
[8]T. W. Donnelly, Phys. Lett. **43B**, 93 (1973); (private communication).
[9]D. A. Krakauer *et al.*, Bull. Am. Phys. Soc. **32**, 1533 (1987).
[10]R. C. Allen *et al.*, Nucl. Instrum. Methods Phys. Res., Sect. A **284**, 347 (1989).
[11]R. L. Burman, M. E. Potter, and E. S. Smith, Nucl. Instrum. Methods Phys. Res. (to be published).
[12]U. Amaldi *et al.*, Phys. Rev. D **36**, 1385 (1987).